

**PARTICLE MANAGEMENT STRATEGIES FOR
ULTRA-HIGH VACUUM ASSEMBLIES**

A Co-op Thesis written for

FERMI NATIONAL ACCELERATOR LABORATORY

and submitted to

KETTERING UNIVERSITY

in partial fulfillment
of the requirements for the
degree of

BACHELOR OF SCIENCE IN MECHANICAL ENGINEERING

by

JOSEPH ANGELO

2016

Student

Employer Thesis Advisor

Faculty Thesis Advisor

DISCLAIMER

This thesis is submitted as partial fulfillment of the graduation requirements of Kettering University needed to obtain a Bachelor of Science in Mechanical Engineering Degree.

The conclusions and opinions expressed in this thesis are those of the student author and do not necessarily represent the position of Kettering University or anyone else affiliated with this culminating undergraduate experience.

PREFACE

This thesis represents the capstone of my five years combined academic work at Kettering University and past work experiences. My Culminating Undergraduate Experience provided the opportunity for me to use the knowledge and skillset learned while at Kettering to manage a project of this magnitude.

Although this thesis represents the compilation of my own efforts, I would like to acknowledge and extend my sincere gratitude to the following persons for their valuable time and assistance, without whom the completion of this thesis would not have been possible:

1. Curtis Baffes, for guiding and supporting me throughout the project, while acting as my Employer Advisor, Fermi National Accelerator Laboratory
2. Kyle Kendziora, for assisting me and instructing me in clean room techniques.
3. Dr. Corneliu Rablau, for his technical assistance and support, while acting as my Faculty Advisor, Kettering University

TABLE OF CONTENTS

DISCLAIMER	2
PREFACE	3
LIST OF ILLUSTRATIONS	5
I. INTRODUCTION	8
Problem Topic	8
Background	8
Methodology	12
Criteria	13
Supporting Material	13
II. CONCLUSIONS & RECOMMENDATIONS	14
Conclusions	14
Recommendations	16
III. EXPERIMENTAL EQUIPMENT AND ENVIRONMENT	19
IV. EXPERIMENTAL METHOD	26
V. DETAILED EXPERIMENTAL RESULTS	28
Galling Between the Washer and the Vacuum Flange	34
Stud Geometry	35
Heat and Sweating	35
Position of the Experimenter and Equipment	36
REFERENCES	37
APPENDICES	38
APPENDIX A: TABLE OF COLLECTED PARTICLE COUNT DATA	39
APPENDIX B: SCANNING ELECTRON MICROSCOPE IMAGES	44

LIST OF ILLUSTRATIONS

Figures

1. Superconducting niobium radio frequency cavity.	9
2. Cryomodule containing SRFCs being installed in Fermilab's CMTF.	10
3. A vacuum assembly using stainless steel and silicon-bronze fasteners.....	11
4. A replacement knee with TiN coating.	12
5. Fermilab's Cryomodule Testing Facility (CMTF).	19
6. The class 10 cleanroom in the CMTF.	20
7. Vacuum spool with conflat flanges on both ends.	21
8. Testing fixture wrapped in clean room plastic.....	21
9. Climet particle counter.....	22
10. Wall port between cleanrooms.....	23
11. Steel, silver, and TiN studs.	24
12. Bolt tightening pattern, from MDC.	27
13. Particle count by process and material.....	29
14. SEM image of a TiN surface with wear particles.	31
15. SEM image of stainless steel surface with wear marks.	32
16. SEM image of silver coated surface with wear marks.....	33
17. Galling damage on a conflat flange.	34

Appendices

B-1. Stainless Steel Thread Tip	45
B-2. Stainless Steel Thread Wall	45
B-3. Stainless Steel Thread Deformity	46

B-4. Stainless Steel Thread.....	46
B-5. Stainless Steel Thread Wall, Spectrometry View.....	47
B-6. Stainless Steel Thread, Spectrometry View.....	47
B-7. Stainless Steel Wear Marks	48
B-8. Stainless Steel Wear Marks Zoom.....	48
B-9. Silver Thread Wall.....	49
B-10. Silver Surface Deformity	49
B-11. Silver Thread.....	50
B-12. Silver Thread Close-up.....	50
B-13. Silver Wear Marks	51
B-14. Silver Wear Close-up.....	51
B-15. TiN Thread Wall.....	52
B-16. TiN Thread Wall Close-up.....	52
B-17. TiN Thread Deformity	53
B-18. TiN Thread Deformity Close-up.....	53
B-19. TiN Thread.....	54
B-20. TiN Thread Close-up	54
B-21. TiN with Stainless Steel Wear Particles	55

Tables

1. Particle Generation Characteristics.....	28
2. Statistical T-test Data.....	30

Appendices

A-1. Stainless Steel Stud Particle Data 40

A-2. Silver Coated Stud Particle Data 41

A-3. TiN Coated Stud Particle Data 42

A-4. Particle Size Data..... 43

I. INTRODUCTION

In the assembly of ultra-high vacuum, particle free devices (UHV/PF), cleanliness is of chief concern. Contaminant particle generation during assembly is a major cause of contamination to sensitive systems. Proper material and coating selections for fasteners can significantly affect the amount of contaminants generated during assembly [1]. Galling is a concern for all clean-room applications, and may also be addressed by material and coating selection.

Problem topic

Fermilab must reduce fastener based particle contamination, galling, and corrosion during the assembly of vacuum fixtures. Fermilab lacks particle generation data from its current assembly methods.

Background

Next-Generation linear particle accelerators (LINACs) will utilize superconducting radio frequency cavities (SRFCs) to accelerate particles at higher gradients (i.e. energy gain per unit length) than are possible with traditional RFCs.

SRFCs, such as the the one in Figure 1, require extreme cleanliness to run effectively, especially at high gradients. Superconducting materials exhibit negligible electrical resistance and significantly reduced impedance when cooled to cryogenic temperatures, below their “critical temperature”, using liquid helium in a Cryostat, pictured in Figure 2. [2] Any non-superconducting material present, including contaminant dust, will heat up when alternating current is put through the superconductor. This heating will cause the resistance and impedance of the superconductor to rise, resulting in further heating. This effect can cascade rapidly,

causing a “quench”, where the entire device is heated beyond its critical temperature, resulting in the shutdown of the device and damage to the equipment. Even small amounts of contamination can cause significant degradation in the effectiveness of the SRFC. [3]



Figure 1. Superconducting niobium radio frequency cavity.

SRFC's are one component of the extensive vacuum system of a particle accelerator. To preserve cleanliness, all components at Fermilab which make contact with the vacuum are cleaned in ultra-sonic baths, blown clean with pure nitrogen, and assembled in a clean room. However, contaminant particles can be generated after cleaning by fastener wear during the assembly of vacuum systems, and are more difficult to detect and remove from the completed system than from individual parts. Therefore, particles generated during assembly are a serious concern in the cleanliness of the system.

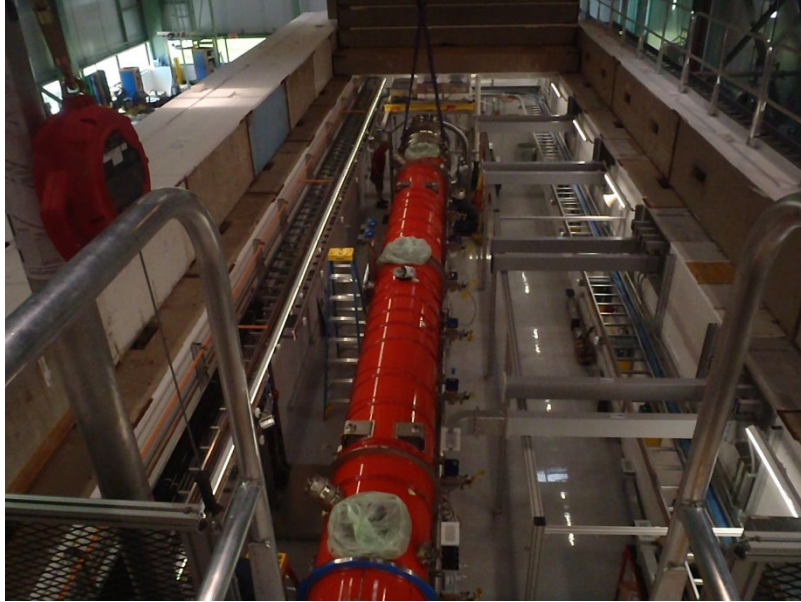


Figure 2. Cryomodule containing SRFCs being installed in Fermilab's CMTF.

Contaminant particles are generated primarily through wear. [1] This wear can be of any form, but this report examines wear through contact erosion, galling, and corrosion. Contact erosion is damaging of a surface by contact with another surface, and is most often controlled by using high hardness materials. Galling is a form of “cold welding”, where two very clean metal surfaces make contact, and may stick together or damage the surfaces as they pull apart. Galling is a common hazard in clean room applications, where the dust and oxide layers that usually protect metal surfaces have been cleaned off. Vacuum makes galling even more likely, as the protective oxide layer which prevents everyday objects from galling cannot form. [4] Corrosion, the oxidation of metals, can result in both particle generation and structural weakening. The moist underground environment and long lifetime of particle accelerators requires that all parts in the accelerator be corrosion resistant.

Several strategies for preventing galling and corrosion are already used in vacuum system fasteners. Stainless Steel/Silicon-Bronze interfaces, pictured in Figure 3, are often used for UHV/PF systems, and silver coatings are used in vacuum systems not sensitive to particle contamination. These methods do not provide significant protection from contact wear, however. Silicon-Bronze and silver are soft metals, and are particularly vulnerable to contact wear. Preventing contact wear requires hard, smooth, lubricious material, such as Titanium-Nitride (TiN) ceramic coating.

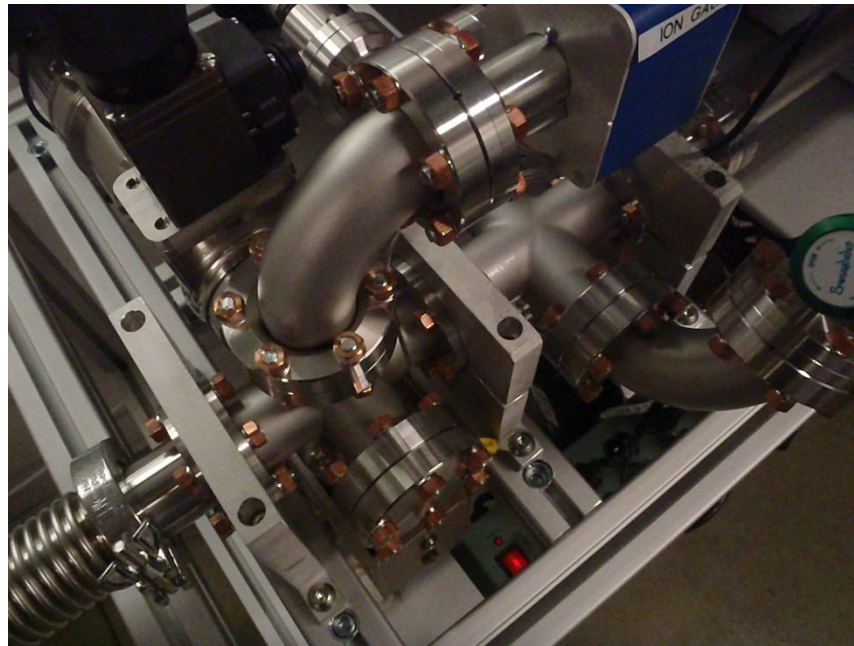


Figure 3. A vacuum assembly using stainless steel and silicon-bronze fasteners.

Titanium-Nitride also has the benefit of being superconducting at the temperatures used in SRFCs. [5] This means that if TiN particles were to contaminate a SRFC, it would be much less likely to undergo quench or quality degradation. TiN is also corrosion resistant, and has proven effective in wear reduction applications, such as

coated drill bits, and in applications where contact particle generation is a serious concern, such as orthopedic implants, like figure 4, where hard particles can cause swelling in adjacent tissue. [6]



Figure 4. A replacement knee with TiN coating.

Methodology

The intent of this project is to compare the particle generation and gall prevention characteristics of stainless steel, silver coated, and TiN coated fasteners. To achieve this goal, the following steps were taken:

- A testing stand was designed to be compatible with cleanroom requirements.
- Data acquisition programs and equipment were obtained and implemented.
- Particle count data was collected during the assembly and disassembly of conflat vacuum flanges.
- Observations of galling and particle generation phenomena were made.
- A Student T-test was applied to the collected particle data to determine the statistical significance of the collected data.

- Samples were placed under a Scanning Electron Microscope to examine particle generation phenomena.

Criteria

To be considered successful, this project must:

- Experimentally determine the particle generation characteristics of stainless steel, silver coated, and titanium nitride coated bolts, when mated with silicon bronze, stainless steel, and stainless steel nuts, respectively
- Determine and provide explanations of particle generation phenomena
- Provide a description of the galling prevention characteristics of the materials tested.

Supporting Material

The following chapters describe the project in greater detail. Chapter II outlines the results and conclusions of the experiment. Chapter III describes the equipment used in the experiment. Chapter IV describes the methodology used in performing the experiment and in the clean-room techniques used. Chapter V describes the phenomena determined to be behind the observed particle generation.

II. CONCLUSIONS & RECOMMENDATIONS

This chapter provides conclusions and recommendations based on the experiments described throughout this thesis. These are presented based on the particle data collected and the qualitative observations made while assembling conflat vacuum flanges with Stainless Steel, Silver coated, and TiN coated fasteners. The conclusions regarding particle count data have been statistically validated using a Student T-test.

Conclusions

The primary purpose of this this thesis was to determine the difference in the Particle generation characteristics of Stainless Steel, Silver coated, and TiN coated fasteners; and to analyze the galling hazards presented by these assembly methods. It has been experimentally proven that:

- Silver coated studs, in conjunction with Stainless Steel nuts, produce fewer contaminant particles than any other configuration, with a mean of 229 particles per bolt.
- Stainless Steel studs produced a mean of 763 particles per bolt
- Titanium Nitride coated studs produced a mean of 4021 particles per bolt. This high count is caused by a high hardness combined with pervasive micrometer scale surface defects
- Galling hazards are nearly uniform for all sample types. Galling did not occur between the stud and nut for any sample, but between the washer and vacuum flange.
- Preventable particle generation is closely related to surface roughness and hardness. It is also caused by washer galling, wrench slipping, sweating, the position of the operator, the number of people in the cleanroom, deformed stud geometry, and contact between the thread of the stud and the inner wall of the bolt hole.

This data contradicts common belief and practice at Fermilab that SS/SB fasteners produce less contamination than Ag/SS configurations. However, the strict requirements

imposed by the T-test render the results of this experiment very compelling. The particle count data can be found in Appendix A, and a statistical analysis can be found in Chapter IV.

When the samples were viewed under the SEM microscope, the surface geometries offered explanations as to the particle generation results. The description of the SEM results can be found in Chapter V, and further SEM images can be found in Appendix B.

A caveat in this test was a slight dimensional difference between the studs tested. The silver studs were approximately one thousandth of an inch narrower than the other studs tested. While this may cast doubt on the conclusion that Ag studs are cleaner than SS studs, it suggests that fastener quality and geometry may make an impact in the particle generation associated with the fastener. However, the performed T-test did not show a statistical difference between the Ag and SS studs during the setup of the flange, where the size difference would be expected to decrease stud-flange contact, and reduce the particle count. Additionally, no literature was found that analyzes the effects of contaminant particle size on damaging effects such as quench. Smaller particles can travel farther through a vacuum, [7] and therefore may be more dangerous than large particles in that respect, but these particles may be less likely to cause a quench than their larger counterparts, as they contain much less material. Most particles generated for each sample were between 0.3um and 0.5um, which matches the results found by Miller [1]. Therefore, while particle size distribution was recorded in this experiment, it is difficult to make a recommendation based off of the collected data. Since each particle, regardless

of size, represents one chance for contamination, all particles were treated equally for the purpose of the statistical analysis.

Recommendations

Based on the above conclusions, these recommendations are made to the Fermi National Accelerator Laboratory:

- Use Silver coated studs with Stainless Steel nuts in all future UHV/PF assemblies.
- Use Washers which are not composed of Stainless Steel in all future UHV/PF assemblies.
- Create an air-conditioning system for the cleanrooms.
- Avoid the use of any titanium nitride in clean-room applications unless coatings with suitable surface characteristics can be found.
- Continue the search for materials and coating with particle reduction properties.
- Determine the importance of particle size in causing quench and quality degradation.
- Write a “Best Practices” document formalizing the methods used to minimize particle contamination during assembly procedure.

The first recommendation, the use of Ag coated studs in UHV/PF applications, is the most direct conclusion of the experiment, and is supported by the particle data collected and its statistical analysis. Implementing this recommendation will reduce the level of contamination found in all future assemblies.

The second recommendation, the use of non-SS washers, will likely yield the largest drop in particle generation of any single action. While the number of galling incidents was not recorded, galling events should be related to pressure between the surfaces [4] and on their cleanliness, both of which will be similar for all sample types per clean room and vacuum supply vendor specification. Therefore, the observations that

galling occurs with significant frequency, independent of coating, and produces large amounts of contaminant, are enough to recommend a change in materials.

The third recommendation is useful both for increasing cleanliness of assembly and cleanroom up-time. Cleanrooms must be kept below a certain temperature to prevent sweat from dripping onto assemblies. Above this temperature, work cannot be feasibly carried out in the cleanroom. However, even below this temperature, sweat may be captured by the operator's breath, and transferred to the assembly. This was repeatedly observed by the operator on the particle counter's display, but the particle counter lacked sufficient recording resolution to capture the phenomenon, which occurred at the rate of breath. The nature of under-construction particle accelerator facilities is one of constant equipment installation. This means that the heat input to the facility is constantly rising, and can quickly render a central air conditioning system insufficient. Therefore, this thesis recommends the use of independent air conditioning systems for all clean rooms.

The fourth recommendation is a caution against using unproven Titanium Nitride coatings. This is supported by the extremely high particle counts seen when testing TiN coated studs. Additionally, the first three sets of data taken, which are not analyzed here, were invalidated by contamination prior to the realization of this phenomena. This recommendation is qualified due to the wide variety of TiN available, and its use in other particle sensitive activities; [8] which suggests that an acceptable TiN coating may still be found.

The fifth recommendation, continuing the search for particle reducing materials and coatings, emphasizes the importance of further study into particle reduction methods. Material considerations have yielded improved contamination mitigation in other

applications, using materials not tested in this thesis. As the equipment and technique required to test for particle generation has already been developed, it should be used to further enhance Fermilab's UHV/PF assembly techniques.

The sixth recommendation, the study of particle size on quench, is important in interpreting the data collected by this experiment. Were large or small particles found to be more dangerous than others, it could significantly impact the conclusions and recommendations made by this thesis.

The seventh and final recommendation, the establishment of a written cleanroom Best Practice, is important for the preservation of the knowledge of particle generation phenomena gained by this experiment, and by future technicians. Additionally, it will aid in the education of future clean room workers, as well as significantly reduce contamination, if all of the recommendations are adhered to. These more general recommendations can be found in Chapter VI.

III. EXPERIMENTAL EQUIPMENT AND ENVIRONMENT

This chapter describes the equipment with which the experiment was performed, and the environment in which it took place.

The experiment took place within the clean room in Fermilab's Cryomodule Testing Facility (CMTF) shown in Figure 5. The cleanroom is ISO Class 4, equivalent to FED Class 10, and denotes a limit of 83 particles 1 μ m or larger per meter cubed. For reference, unfiltered "room air" contains about 8,000,000 such particles. [9]



Figure 5. Fermilab's Cryomodule Testing Facility (CMTF).

This room, shown in Figure 6, was nested within a Class 100 and a Class 10,000 clean room. To enter the area around the clean rooms required boot covers, and stepping over adhesive pads. To enter the Class 10,000 room required a lab coat, gloves, and

hair/beard nets. The class 100 and class 10 rooms required full-body cleanroom suits, as well as a second pair of boot covers and gloves covering the first pair, and a face mask and hood which covered the initial hair nets. All clean room entrances were immediately preceded and succeeded by adhesive floor pads, intended to remove dust from the bottoms of shoes or boot covers. The clean rooms were positively pressurized to prevent the entry of particles, and separated by doors or plastic curtains. All of the cleanrooms have constant downward airflow, to prevent the spread of airborne particles.



Figure 6. The class 10 cleanroom in the CMTF.

The spools and flanges (Figure 7) used in the experiment were purchased from MDC. They were cleaned to particle-free status in the CMTF cleanroom at Fermilab, and sealed in plastic clean room wrap until use. The testing stand was blown clean with nitrogen, wiped down with cleanroom wipes, sealed in cleanroom wrap, and kept within the wrap for the duration of the experiment, except for the pipe clamps (Figure 8).

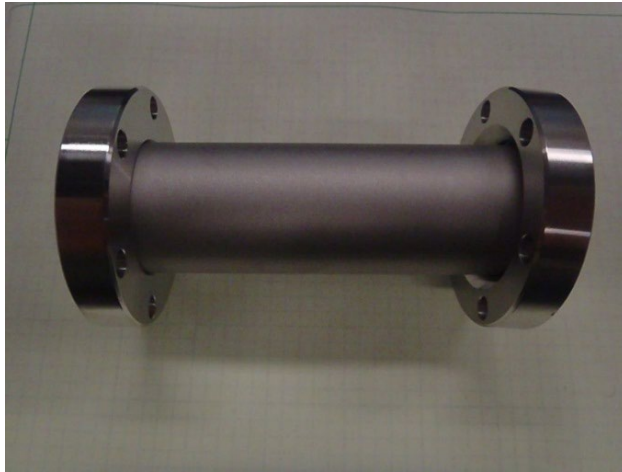


Figure 7. Vacuum spool with conflat flanges on both ends.

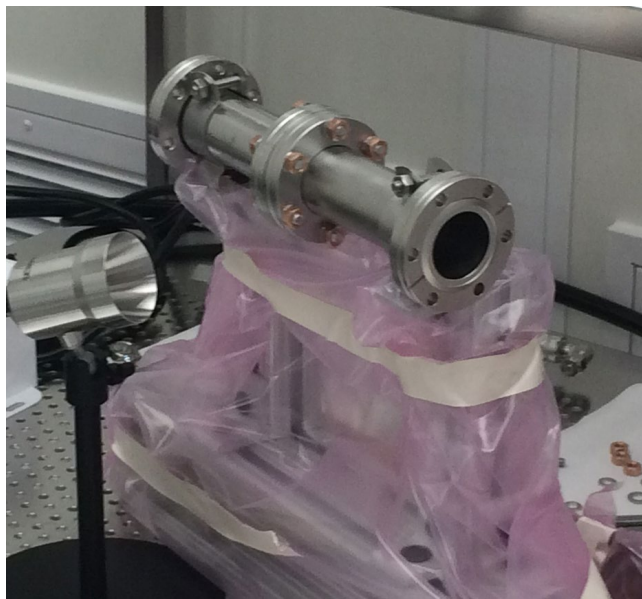


Figure 8. Testing fixture wrapped in clean room plastic.

The torque watch was cleaned and bagged in a similar way, with only the socket of the wrench outside of the bag. The holes in the bag to allow the operational parts of the equipment to protrude were sealed with cleanroom tape. Copper gaskets were purchased from MDC, and arrived in individual plastic clean room packaging. They were wiped

with cleanroom wipes after being removed from their packaging in the class 10 clean room, which technician experience has shown to be sufficient for particle free status.

The device used to collect particle count data was a Climet-750c particle counter, shown in Figure 9. It consists of a sampling horn, which intakes air, a body which detects particles, filters the exhaust, and provides a readout, and a hose to connect the two.



Figure 9. Climet particle counter.

The counter is capable of detecting particles from .1 microns in diameter to 5 microns in diameter, and can detect and record the size of individual particles. It classes particles into size ranges, >5um, 1.0-5.0um, .5um-1um, and .3um-.5um. The intake rate of the counter is 75 liters per minute, and the maximum resolution available is one sample every 4 liters. In practice, this translates to 4-5 seconds per sample. The counter was connected to a laptop via a serial cable. The serial cable was passed from the body of

the counter in the Class 10 room, through two clean room wall ports (Figure 10), and into a laptop in the class 10,000 room.



Figure 10. Wall port between cleanrooms

Data was not fed constantly to the laptop, but was stored on the counter until it was manually downloaded. The sampling horn of the counter was placed below and pointed towards the bolt nearest the operator. This, combined with the downward airflow of the cleanroom, creates a sufficiently strong air current to ensure that the majority of the particles are detected by the counter. The counter was installed in the cleanroom long before the tenure of the experimenter, and its cleaning methodology is not known.

Other equipment used includes a 0-500 N-m torque watch, a crescent wrench, clean room wipes, various wrenches, and the cleanroom's nitrogen gun system, which uses a stream of pure nitrogen gas to clean particles from surfaces.

The samples (Figure 11) were 1-7/8" long 1/4-28 threaded studs, coupled with two nuts and two washers each.



Figure 11. Steel, silver, and TiN studs.

Stainless Steel, electro-polished studs were purchased from JT Industries, half of which were subsequently coated with TiN by Surface Solutions to a nominal thickness of 2um, according to AMS2444, Class 1 specification. The Silver studs were purchased uncoated from McMaster-Carr, and coated with silver by Krell Labs to AMS 2010 standard, with a max thickness of 5um.

All samples were cleaned to UHV (not UHV/PF) spec in the CMTF cleanroom, using ultrasonic baths and nitrogen guns. The studs obtained from JT Industries were found to have some irregularities and deformations on the tips of their threads, as well as to be slightly thicker than their McMaster counterparts. These were mitigated as much as

possible by careful visual inspection and sample selection, as well as by operator dexterity.

IV. EXPERIMENTAL METHOD

This chapter details the method used to collect particle count data from the assembly of conflat vacuum flanges when using fasteners of different materials. It also describes deviations from the method, and actions taken to correct any errors.

1. The vacuum flanges were placed in the pipe clamps of the testing stand, wiped down, and blown with nitrogen until the particle counter indicated a zero count.
2. The samples to be used to affix the flange were chosen, and the copper gasket removed from its sleeve and wiped clean.
3. The counter was reset, and began to sample experimental data.
4. Two studs were inserted into the bolt holes closest to the operator, with washers and nuts finger-tightened on. The operator attempted to make as little contact with the sides of the bolt holes as possible, and to perform the experiment as quickly as possible, to minimize contamination from the operator's gloves.
5. The flanges were rotated to place the two studs in the lowest positions. The flange was separated slightly, and the copper gasket was dropped in.
6. The remaining samples were inserted into the flange. After each insertion, the flange was rotated to place the next bolt hole closest to the operator. Any particles appearing to arise from this rotation were noted and removed from the data analysis.
7. The samples were tightened to 120in-lbs in a star pattern as per MDC spec and shown in Figure 12. However, each sample was tightened to full load in one wrench turn, as opposed to evenly and gradually, as specified by MDC. This was to prevent cross-contamination, and to perform the experiment within a reasonable timeframe.

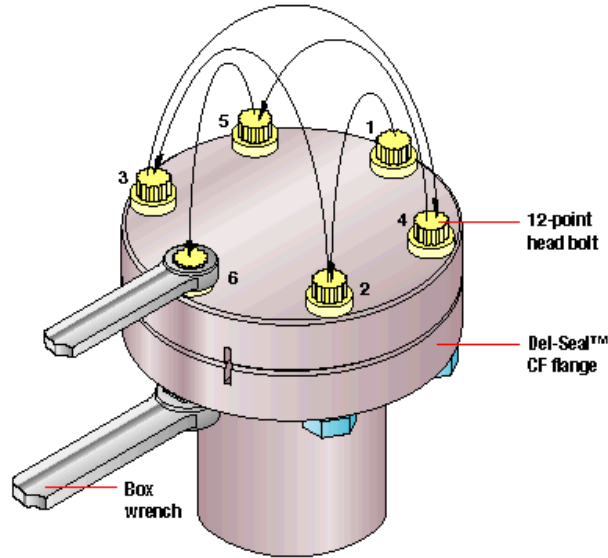


Figure 12. Bolt tightening pattern, from MDC.

8. The particle counter sampling horn was placed at the end of the spool, and nitrogen blown in the opposite end until a zero count was achieved.
9. The sampling horn was replaced under the vacuum flange, and the samples were loosened and removed in reverse of the order they were tightened in.
10. The flange was separated slightly to remove the gasket.
11. The sampling horn was placed at the end of the spool, and nitrogen blown into the opposite end of the spool until a zero count was achieved.
12. The flange and fixture were wiped down and blown clean.
13. The collected data was uploaded to the laptop, and statistically processed.
14. The samples were sealed in cleanroom plastic, and select samples sent to the SEM lab for examination.

The raw particle count data was grouped into samples. Adequate time was given between the testing of each sample to allow for clear interpretation. The sample data was collected, averaged, and applied to a Student T-test. The details of the statistical analysis can be found in Chapter V.

V. DETAILED EXPERIMENTAL RESULTS

This chapter details the quantitative and qualitative characteristics of the experimental data. It describes both the data collected from the particle counter, images collected from the SEM, and observations made by the experimenter. The mean values of particles generated per bolt are seen in Table 1 and Figure 14.

Table 1

Particle Generation Characteristics

Sample Type	SS Particle Count	Ag Particle Count	TiN Particle Count
Average total number of particles detected	763	229	4021
...during bolt insertion	40	27	519
...during bolt tightening	140	51	1415
...during disassembly	583	160	2555

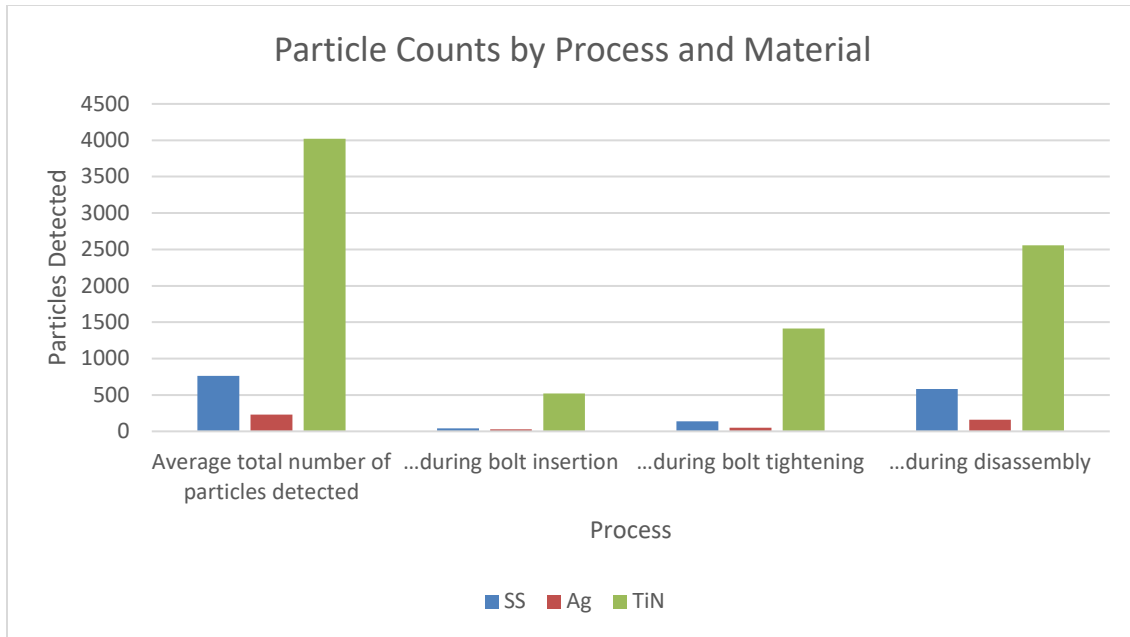


Figure 13. Particle count by process and material.

It can be seen that Ag bolts are the most cleanly, followed by SS, which are followed by TiN. The Test Statistics for the mean values are also found in Table 2. The test statistic is a measure used in a T-test in a manner similar to a standard deviation. To refute a null hypothesis; in this case, that Ag or TiN studs will generate the same amount of particles as SS studs, the means of the two samples must be a certain number of test statistics apart. The test statistic is determined by

$$T = \frac{\bar{X}_1 - \bar{X}_2}{sp \sqrt{\frac{1}{N_1} + \frac{1}{N_2}}}$$

Eq. 1

Were \bar{X}_1 and \bar{X}_2 are the mean values of the two populations being compared, N_1 and N_2 are the number of samples in each population, and sp is a pooled standard deviation determined by:

$$sp = \sqrt{\frac{(N_1 - 1)sp_1^2 + (N_2 - 1)sp_2^2}{N_1 + N_2 - 2}}$$

Eq. 2

The absolute value of the test statistic required to refute the null hypothesis is known as the critical value, and is determined by table. It can be seen in Table 2 that the null hypothesis was refuted for all categories of the TiN experiment, including particles generated during setup, tightening, disassembly, and the sum of the previous three categories, and for all categories of the Ag experiment excepting the setup.

Table 2

Statistical T-Test Data

Sample Type	Ag	TiN
Critical Value	2.05	2.07
T-Statistic, Total	5.45	5.05
T-Statistic, Setup	1.51	3.27
T-Statistic, Tightening	2.53	2.71
T-Statistic, Disassembly	4.09	3.20

It should be noted that the T-test imposes very strict requirements on the rejection of a null hypothesis, strengthening these results. On the other hand, were a T-test to fail

to refute a null hypothesis, the high bar that the T-test sets means that it does not necessarily prove the null hypothesis.

The samples were put under a SEM to determine the characteristics of their wear patterns, and to determine the reason for the high particle counts generated by the TiN studs, and the lower than expected Ag stud particle counts. The TiN studs were found to have a very rough, bumpy surface, which allowed the hard ceramic of the stud to wear away the relatively soft steel of the nut. Figure 16 shows the surface of a TiN stud.

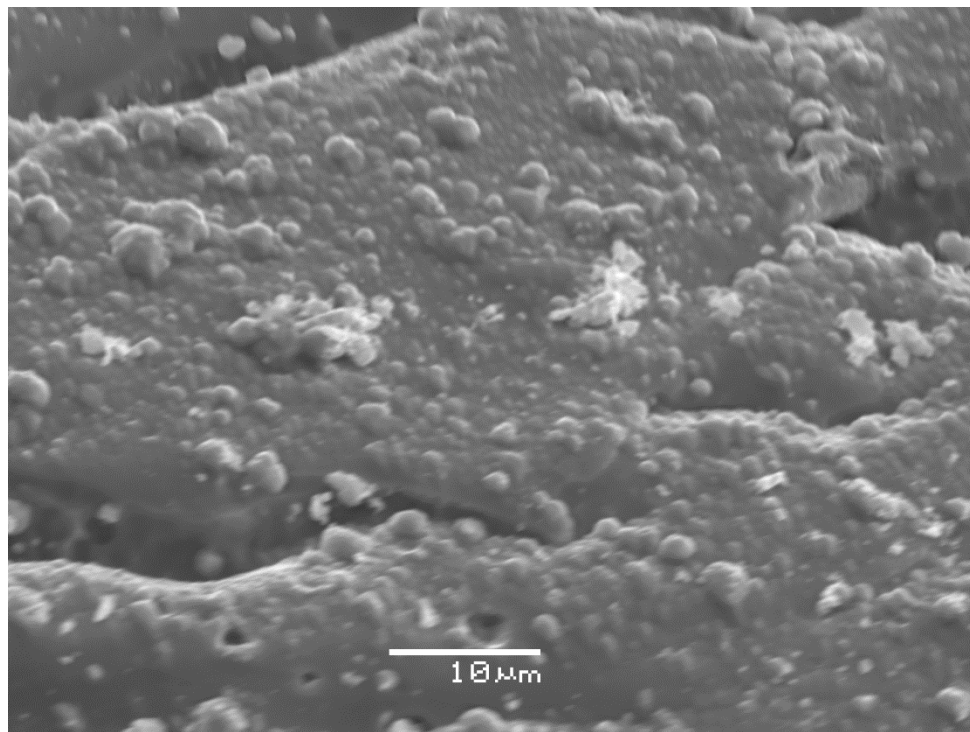


Figure 14. SEM image of a TiN surface with wear particles.

The white flecks seen in Figure 16 were determined to be flakes of steel by X-ray spectroscopy performed in the SEM. In this case, we determine that the hardness of the ceramic did not mitigate particle generation as expected, but greatly increased it. It may be that the relative material hardness of the materials in contact is a more reliable

predictor of particle generation. These images show that the use of TiN studs does not result in TiN particles, but in Steel particles, eliminating the hope that using TiN would produce harmless superconducting contamination. Mubarak states that the TiN particles seen in Figure 16 are a common hazard during the sputtered Physical Vapor Deposition (PVD) processes that is used to apply the TiN coat.[10] However, there are many processes used to produce TiN coatings, many of which are optimized to reduce the macro-particles seen in Figure 16. Therefore, it is imaginable that a process could be selected that would result in fewer TiN macro particles, and less contamination generation.

The comparison of the SS and Ag coated studs gives insights as to why the Ag outperformed the SS. Gouge marks and clear signs of material removal on a SS stud can be seen in Figure 17.

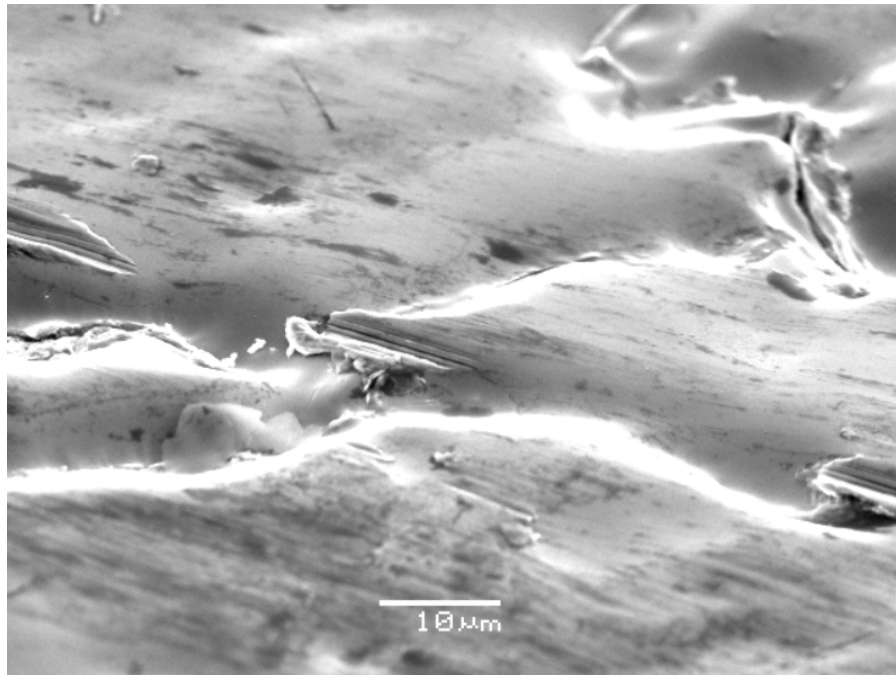


Figure 15. SEM image of stainless steel surface with wear marks.

Wear marks can also be seen on an Ag coated stud in Figure 18, but the raised area and excess material around the wear marks indicates a ploughing wear mechanism , and that much of the material was retained. It may be that the softer and more ductile silver resulted in reduced material removal for the same type of abrasion.

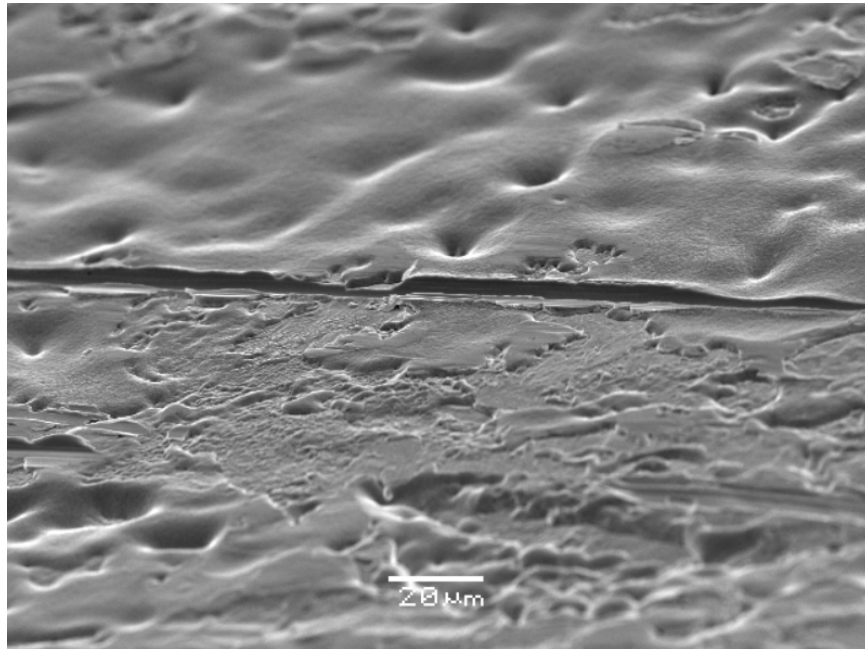


Figure 16. SEM image of silver coated surface with wear marks.

All of the above images were compared with images from unused samples, which can be found in Appendix B.

The following is a list of phenomena that have been seen to generate contaminant particles, and recommendations for their mitigation. These are not necessarily reflected in the data, due to a lack of data acquisition resolution, and their unexpectedness.

Galling Between the Washer and the Vacuum Flange

One of the purposes of protective coatings and of using dissimilar materials in UHV/PF assemblies is to prevent galling. If a stud and nut gall together, they can become impossible to remove by hand, making repairs to the system difficult or impossible. Galling can also make cleaned fasteners unreasonably hard to assemble. All the material combinations examined in this experiment completely eliminated galling between the stud and nut. However, galling did occur between the SS washers and the SS vacuum flange, the result of which is shown in Figure 19, as well as between nuts and washers.

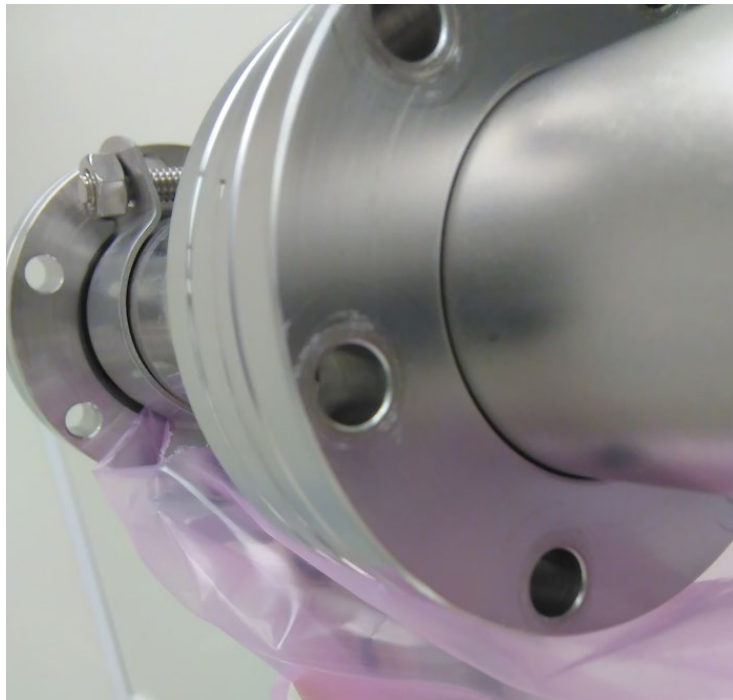


Figure 17. Galling damage on a conflat flange.

Galling occurred both during and after tightening, which were detected by “pinging” sounds made when the washer broke free, and was accompanied by significant spikes in particle generation. This was one of the most significant and easily mitigated

sources of particle generation. It is also a more dangerous form of particle generation than previously thought, due to breakages occurring during assembly as well as disassembly. Fermilab should immediately implement the use of non-SS washers, to reduce particle contamination from galling.

Stud Geometry

A major source of particle generation is the “sawing” action of the threads of the studs against the sides of the vacuum flanges bolt holes. The more precisely the bolt could be inserted, the fewer particles were produced. This was one reason for the low particle counts of the Ag coated studs, their slightly narrower shape aided in stud insertion. Similarly, higher quality stud ends resulted in easier mating of the stud and nut. The amount of time that the operator keeps his hands near a fixture is a significant cause of particle generation. The more quickly the fasteners can be mated, the fewer particles will get onto the assembly. Fermilab should begin sourcing their fasteners from reliable, high quality vendors to mitigate particle generation and contamination. Similarly, a softer barrier, such as cleanroom plastic, could be wrapped around the stud during insertion.

Heat and Sweating

Cleanrooms must be below a certain temperature to operate, above which the sweat of the operator poses a risk to the cleanliness of the UHV/PF assembly. However, sweat contamination can occur below this temperature, by airborne particle picked up by air currents and the operator’s breathe. This was observed by the experimenter, when hot days produced a rate-of-breath oscillation in the particle count display. Unfortunately, the recording resolution was lower than the display resolution, and this phenomena could not

be captured in the data. Fermilab should implement independent air conditioning systems for the cleanrooms to increase their uptime and to prevent particle contamination.

Position of the Experimenter and Equipment

Due to gravity and the downward airflow of the cleanroom, contaminants are much more likely to reach the assembly if they come from above, such as when the operator must reach over the workstation. This is currently mitigated by having the operator be always seated while working, and by the operators diligence in not reaching over the assembly unless absolutely necessary. However, the arrangement of the cleanroom work stations is such that it can be difficult to prevent contamination of the assembly while working with other objects, such as while cleaning gaskets and selecting samples. It was also difficult for the experimenter to seat himself low enough to prevent accidental contamination. If the workstation were redesigned such that the critical assembly was significantly separated from the storage space for the tools and parts to be used, contamination from airborne particles would be reduced.

REFERENCES

- [1] R. J. Miller, "Mechanisms of contaminant particle production, migration, and adhesion," *Journal of Vacuum Science & Technology A: Vacuum, Surfaces, and Films*, vol. 6, no. 3, p. 2097, May 1988.
- [2] S. P, "Basic Principles of RF Superconductivity and Superconducting Cavities," in *11th Workshop on RF Superconductivity*, 2003.
- [3] D. A, R. A, and C. L, "Model for Initiation of Quality Factor Degradation at High Accelerating Fields in Superconducting Radio-frequency Cavities," *Superconductor Science and Technology*, no. 23, 2010.
- [4] K. H, "Galling Behaviour and its tests in press forming of autobody parts," Unpublished Master's Thesis, 2008
- [5] S. Ohya *et al.*, "Room temperature deposition of sputtered TiN films for superconducting coplanar waveguide resonators," *Superconductor Science and Technology*, vol. 27, no. 1, p. 015009, Dec. 2013.
- [6] F. A, L. P, and H. S, "The ionization of metal.," *Journal of Bone and Joint Surgery*, no. 42, pp. 77–90, 1960.
- [7] J. M. Jimenez, J. L. Dorier, and N. Hilleret, "Measurements of particulate contamination and migration under vacuum using a large sensitive area particle counter," *Vacuum*, vol. 53, no. 1-2, pp. 329–333, May 1999.
- [8] R. P. van Hove, I. N. Sierevelt, B. J. van Royen, and P. A. Nolte, "Titanium-Nitride coating of Orthopaedic Implants: A review of the literature," *BioMed Research International*, vol. 2015, pp. 1–9, 2015.
- [9] *Cleanrooms and associated controlled environments*, International Standards Organization Standard ISO/IEC 14644-1:2015, 2015.
- [10] M. A, H. E, and T. M, "Review of Physical Vapor Deposition (PVD) Techniques for Hard Coating.," *Jurnal Mekanikal*, no. 20, pp. 42–51, Dec. 2005.

APPENDICES

APPENDIX A

**TABLE OF COLLECTED PARTICLE
COUNT DATA**

Table A-1

Stainless Steel Stud Particle Data

Stainless Steel				
Flange 1	Setup	Trial	Disassembly	Total
Sample 1	49	69	739	857
Sample 2	55	88	809	952
Sample 3	42	495	376	913
Sample 4	51	191	204	446
Sample 5	41	254	532	827
Sample 6	18	43	1278	1339
AVG	42.66667	190	656.333333	889
Flange 2				
Sample 1	67	177	211	455
Sample 2	94	173	351	618
Sample 3	24	62	409	495
Sample 4	6	35	494	535
Sample 5	11	76	527	614
Sample 6	24	19	1064	1107
AVG	37.66667	90.33333	509.333333	637.3333
Average	40.16667	140.1667	582.833333	763.1667
Std.Dev	25.35147	133.8519	331.995299	283.429
Pooled Std. Dev.	N/A	N/A	N/A	N/A
T Statistic	N/A	N/A	N/A	N/A
Critical Value	N/A	N/A	N/A	N/A
Null Hypothesis Rejected?	N/A	N/A	N/A	N/A

Table A-2

Silver Coated Stud Particle Data

Silver Coated				
Flange 1	Setup	Trial	Disassembly	Total
Sample 1	40	155	356	551
Sample 2	31	39	268	338
Sample 3	52	20	94	166
Sample 4	20	53	16	89
Sample 5	57	32	NA	89
Sample 6	24	99	832	955
AVG	37.333333	66.333333	313.2	364.6667
Flange 2				
Sample 1	70	44	19	133
Sample 2	36	104	49	189
Sample 3	4	145	91	240
Sample 4	3	52	22	77
Sample 5	0	51	445	496
Sample 6	10	52	188	250
AVG	20.5	74.66667	135.6666667	230.8333
Flange 3				
Sample 1	44	13	8	65
Sample 2	16	18	21	55
Sample 3	6	14	67	87
Sample 4	50	10	11	71
Sample 5	14	13	109	136
Sample 6	3	7	119	129
AVG	22.16667	12.5	55.83333333	90.5
Average	26.66667	51.16667	159.7058824	228.6667
Std.Dev	21.61699	45.53505	215.3960784	231.6854
Pooled Std. Dev.	24.03016	94.52882	277.4300097	262.838
T Statistic	-1.50745	-2.52634	-4.09245595	-5.45665
Critical Value	2.048	2.048	2.048	2.048
Null Hypothesis Rejected?	No	Yes	Yes	Yes

Table A-3

TiN Coated Stud Particle Data

TiN Coated				
Flange 1	Setup	Trial	Disassembly	Total
Sample 1	560	11	1230	1801
Sample 2	2203	209	529	2941
Sample 3	194	39	798	1031
Sample 4	494	418	2921	3833
Sample 5	147	117	3405	3669
Sample 6	255	1743	2162	4160
AVG	642.1667	422.8333	1840.833333	2905.833
Flange 2				
Sample 1	500	1641	675	2816
Sample 2	231	261	7486	7978
Sample 3	547	403	2460	3410
Sample 4	1136	1459	971	3566
Sample 5	405	2413	3712	6530
Sample 6	293	2310	5024	7627
AVG	518.6667	1414.5	3388	5321.167
Average	585.1667	880.5256	2554.910256	4020.603
Std.Dev	550.6793	893.5931	2005.62004	2110.403
Pooled Std. Dev.	408.8273	670.0998	1507.648149	1579.168
T Statistic	3.265369	2.706316	3.204051421	5.052695
Critical Value	2.074	2.074	2.074	2.074
Null Hypothesis Rejected?	Yes	Yes	Yes	Yes

Table A-4

Particle Size Data

	Particle Size as Percentage of Total Particles Generated			
Flange #	0.3-0.5 μm	0.5-1.0 μm	1.0-5.0 μm	$\geq 5.0 \mu\text{m}$
Steel				
6	50.67%	29.85%	17.41%	2.07%
8	55.47%	28.08%	14.75%	1.70%
average	53.07%	28.96%	16.08%	1.89%
Silver				
4	55.51%	25.87%	16.02%	2.60%
5	65.19%	22.43%	10.70%	1.68%
7	64.50%	23.41%	10.75%	1.34%
average	61.73%	23.90%	12.49%	1.87%
TiN				
9	67.61%	23.45%	8.35%	0.59%
10	63.62%	24.68%	10.98%	0.71%
average	65.61%	24.06%	9.67%	0.65%

APPENDIX B

SCANNING ELECTRON MICROSCOPE IMAGES

Stainless Steel

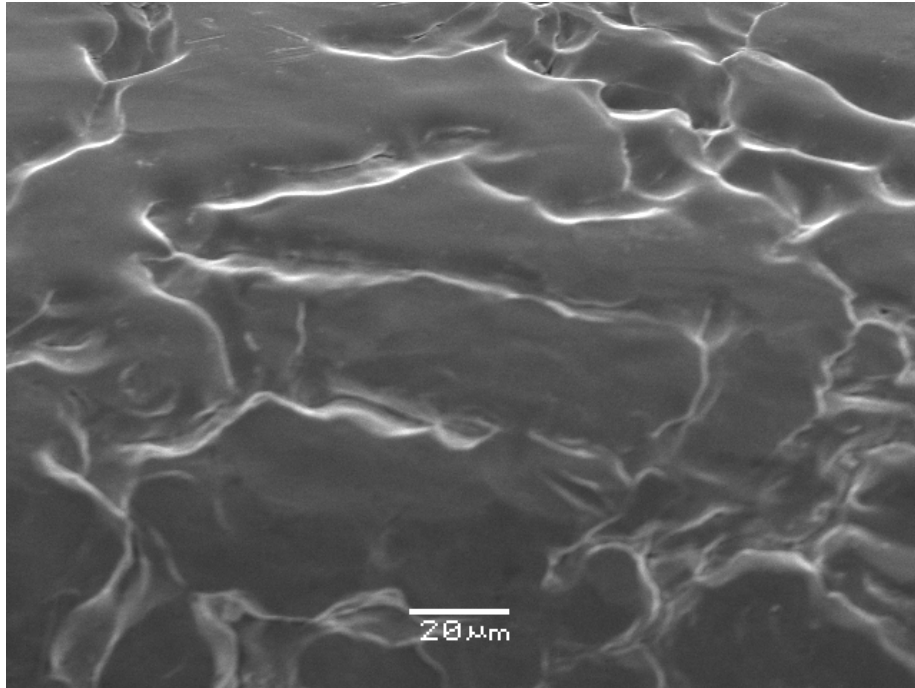


Figure B-1. Stainless Steel Thread Tip

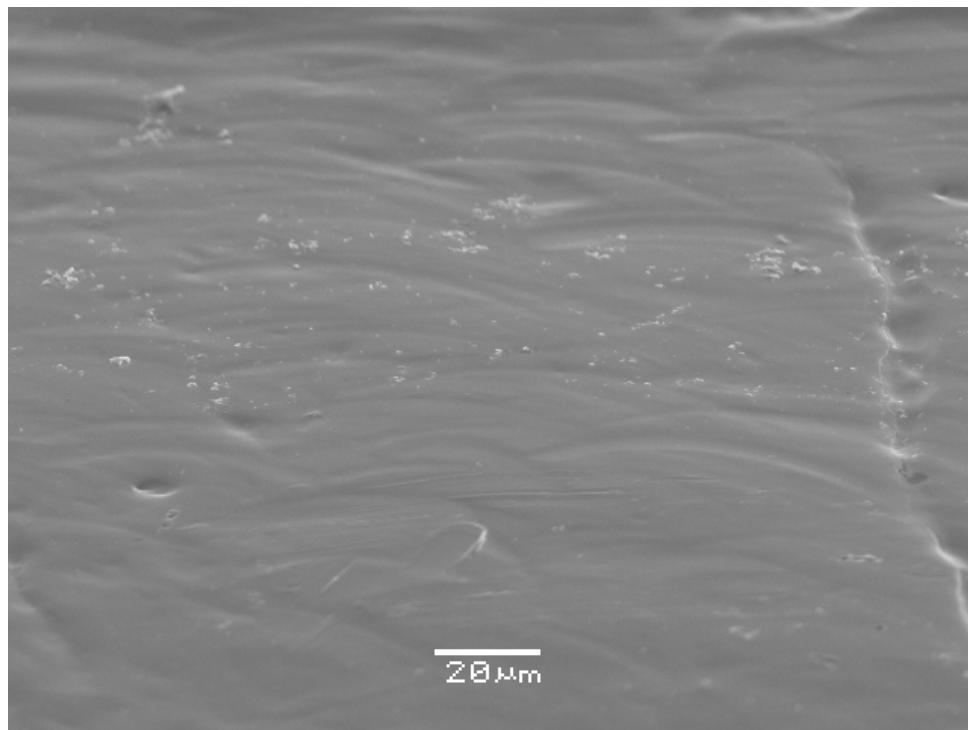


Figure B-2. Stainless Steel Thread Wall

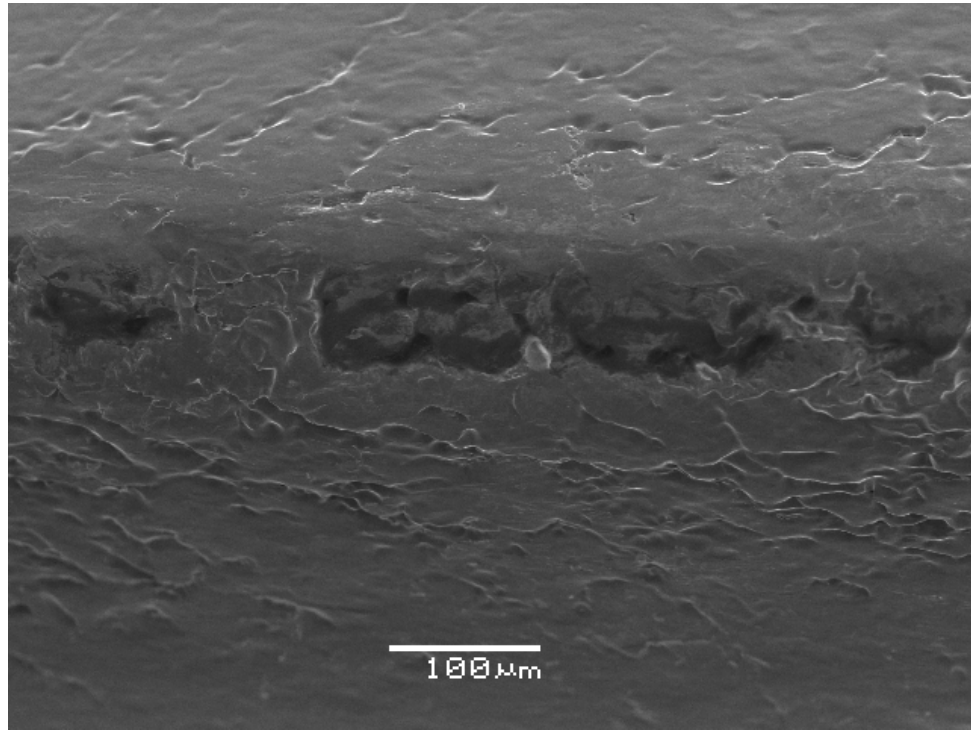


Figure B-3. Stainless Steel Thread Deformity

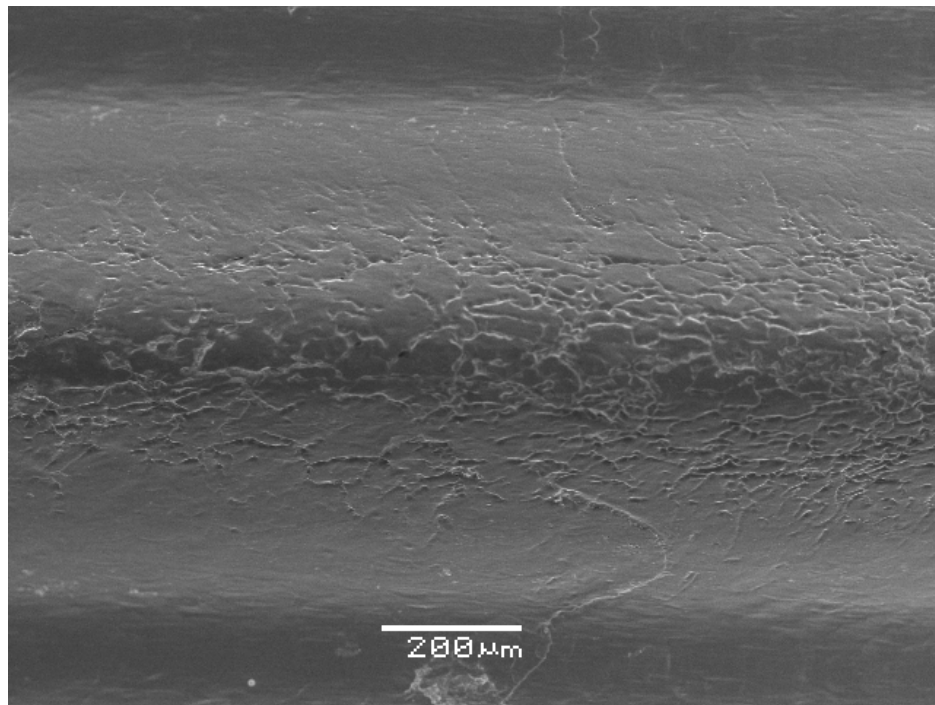


Figure B-4. Stainless Steel Thread

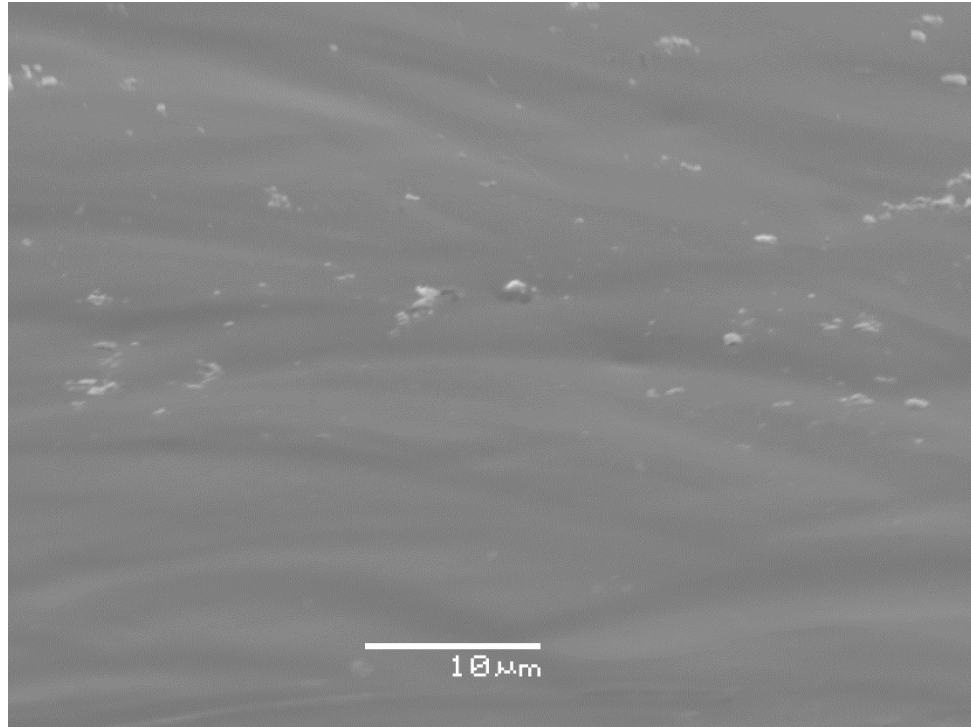


Figure B-5. Stainless Steel Thread Wall, Spectrometry View

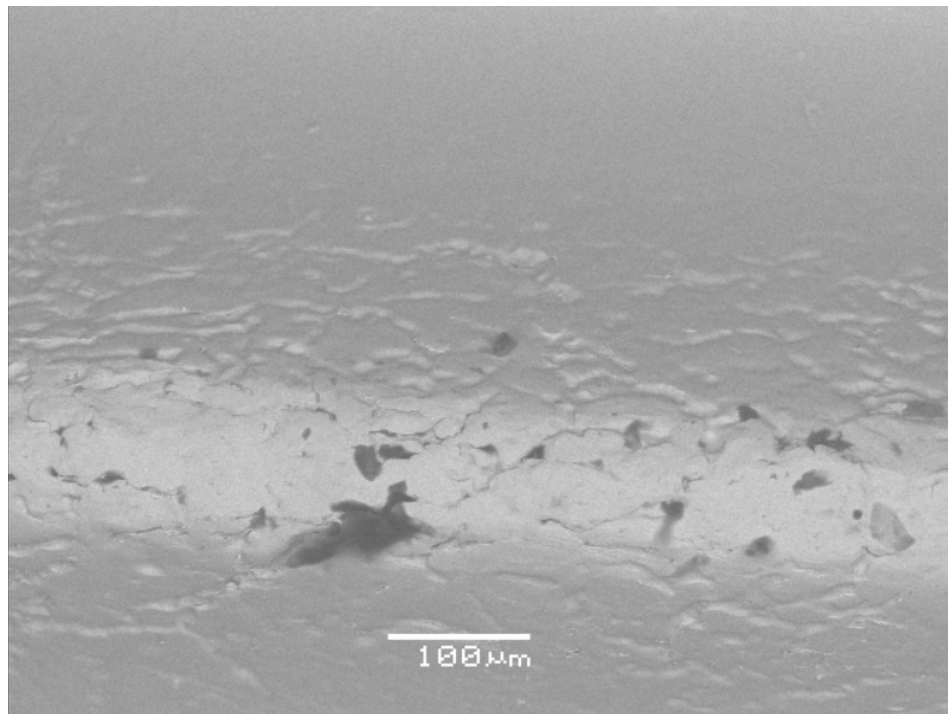


Figure B-6. Stainless Steel Thread, Spectrometry View

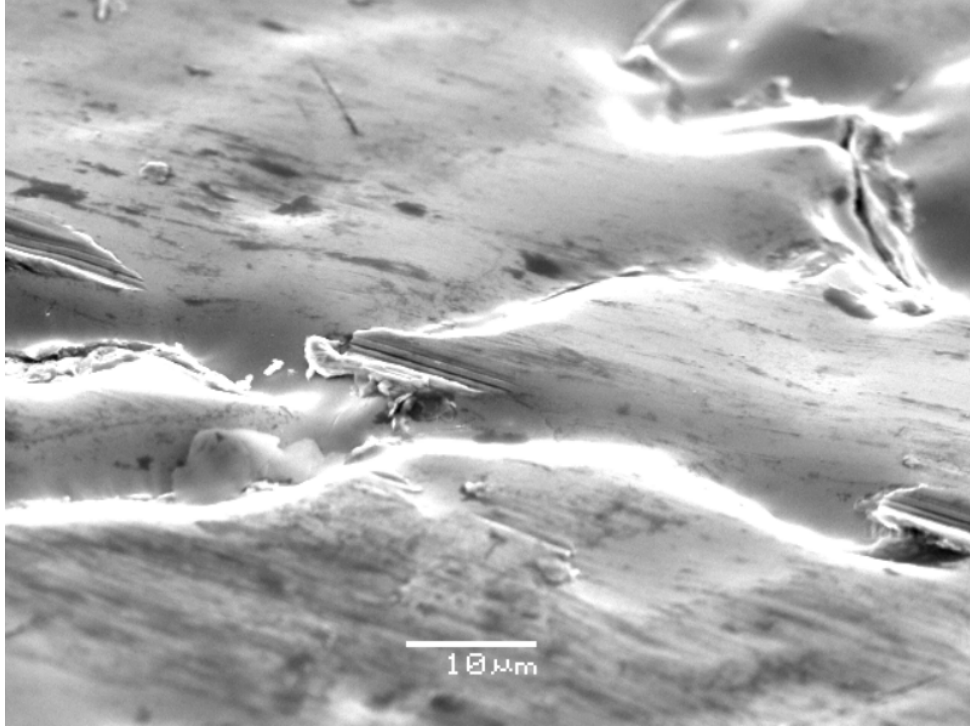


Figure B-7. Stainless Steel Wear Marks

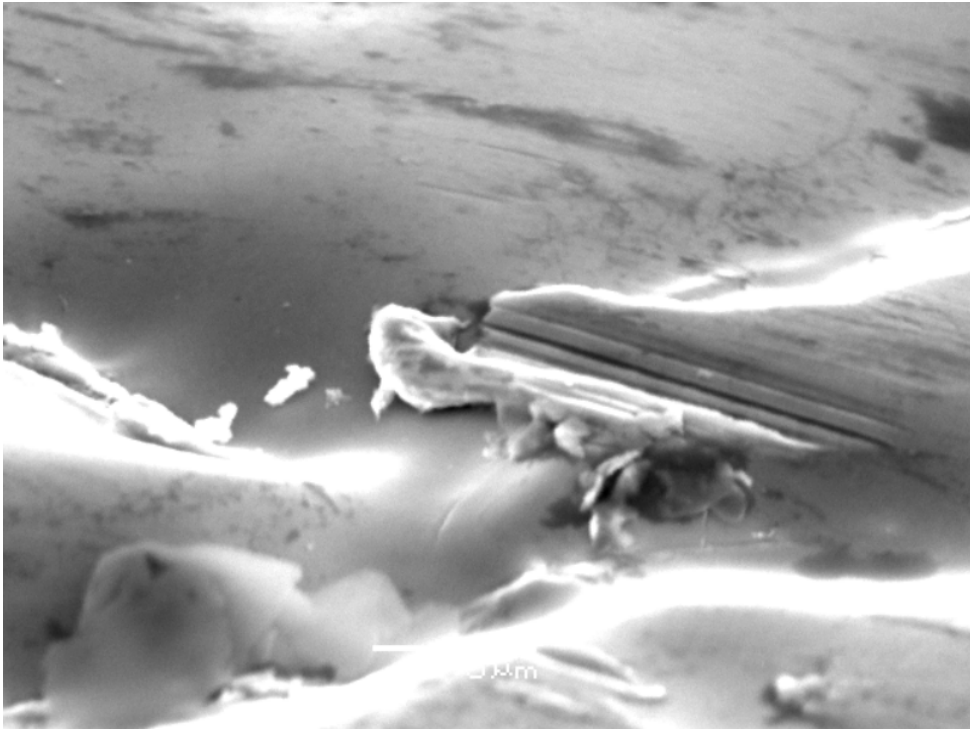


Figure B-8. Stainless Steel Wear Marks Zoom

Silver Coated

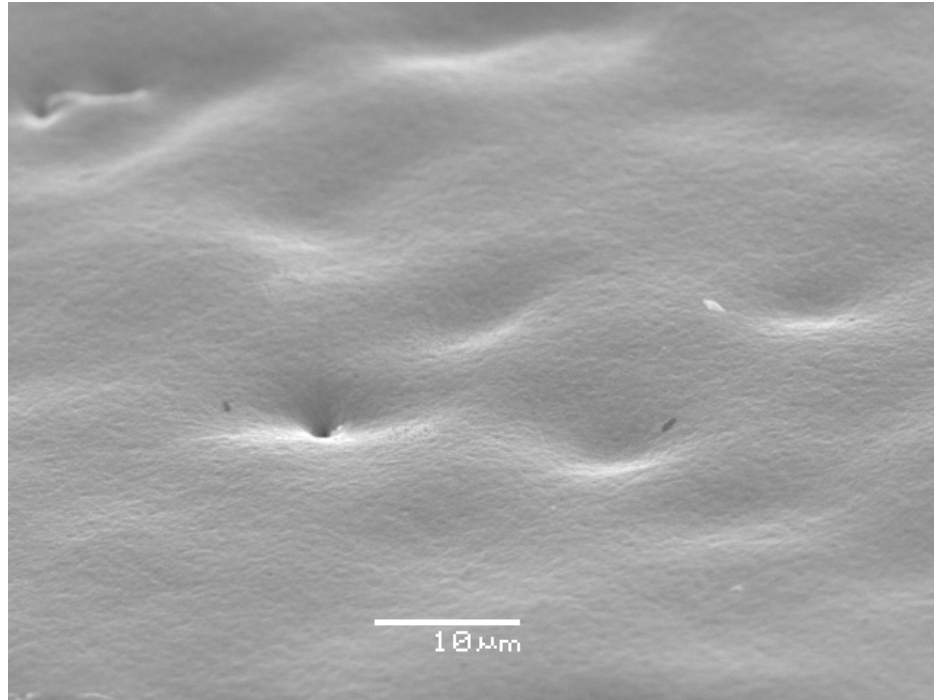


Figure B-9. Silver Thread Wall

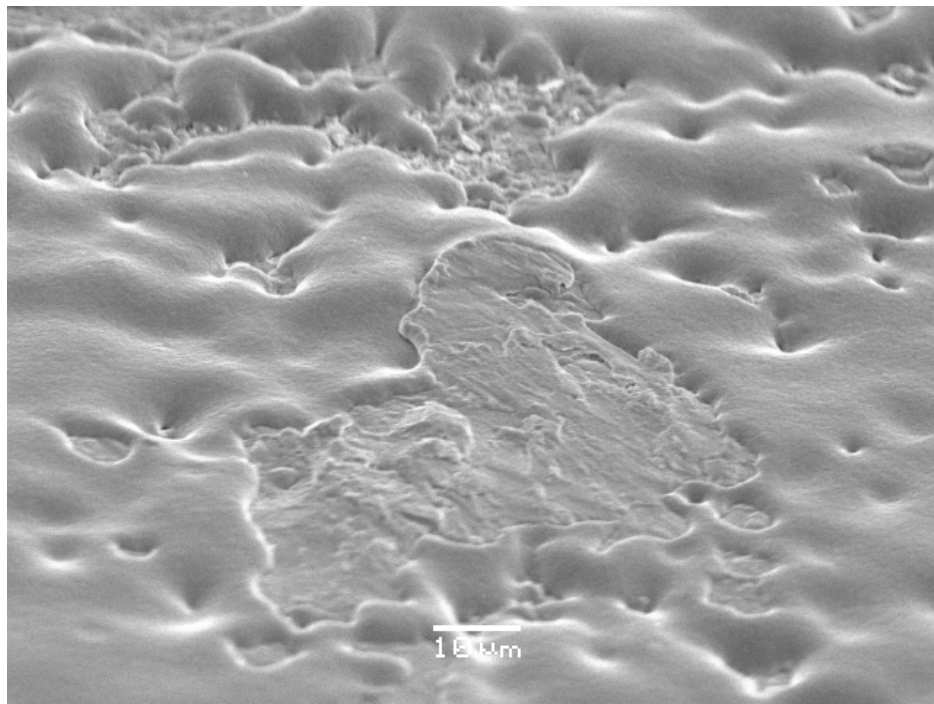


Figure B-10. Silver Surface Deformity



Figure B-11. Silver Thread

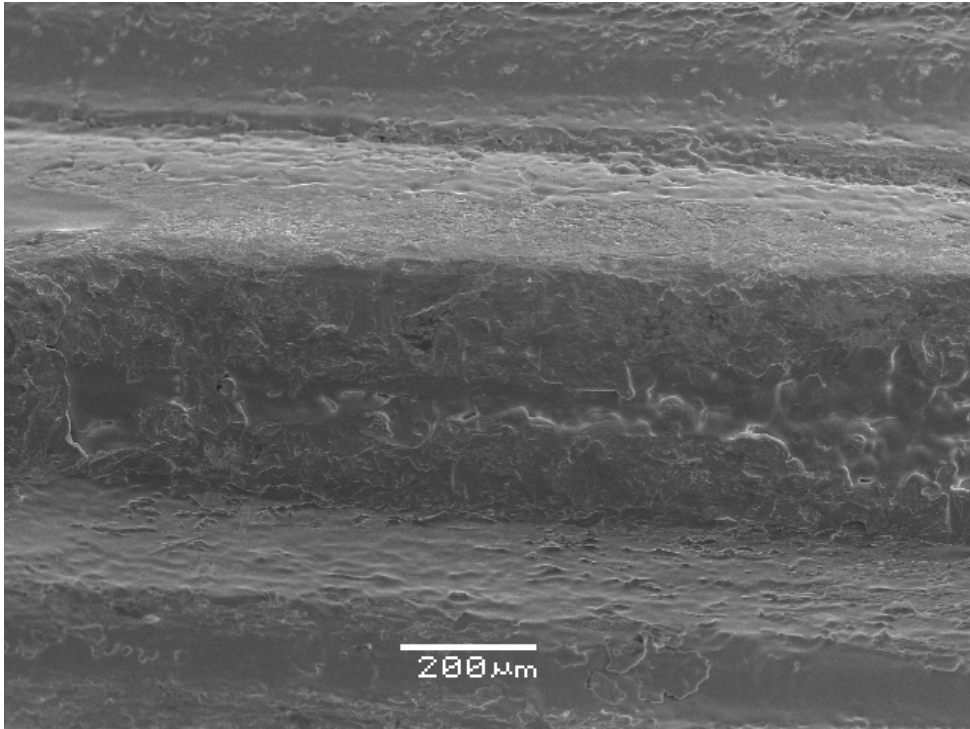


Figure B-12. Silver Thread Close-up

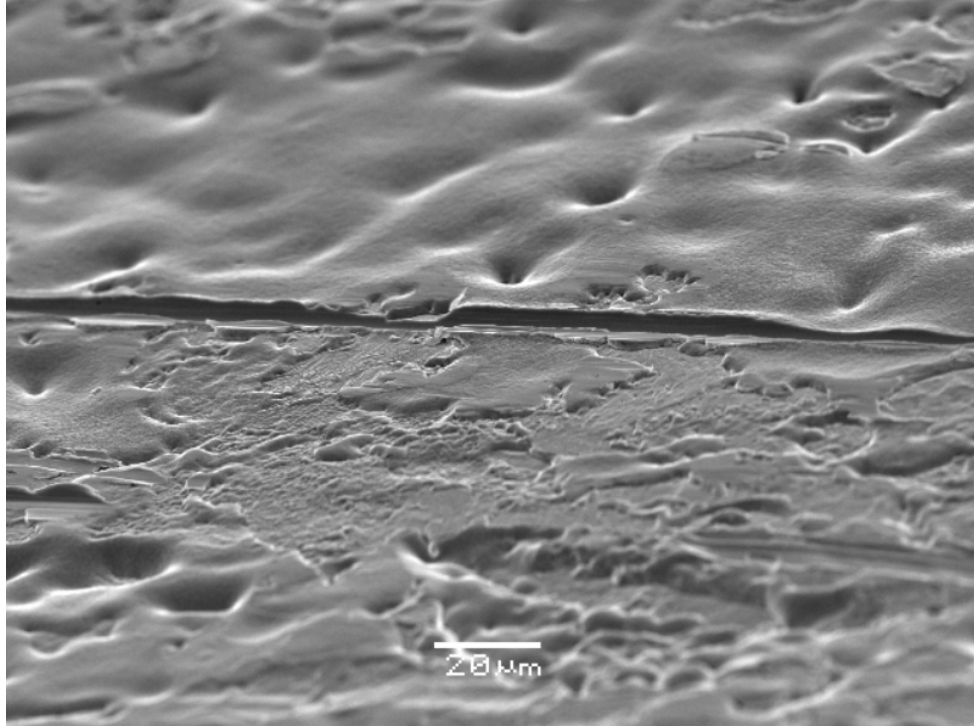


Figure B-13. Silver Wear Marks

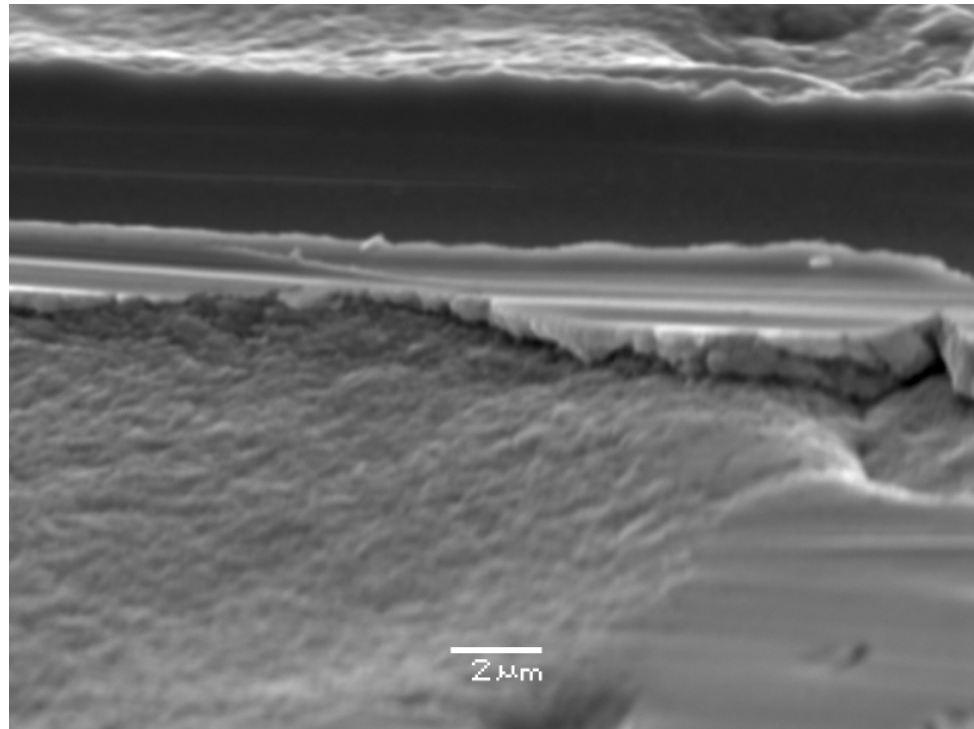


Figure B-14. Silver Wear Close-up

TiN Coated

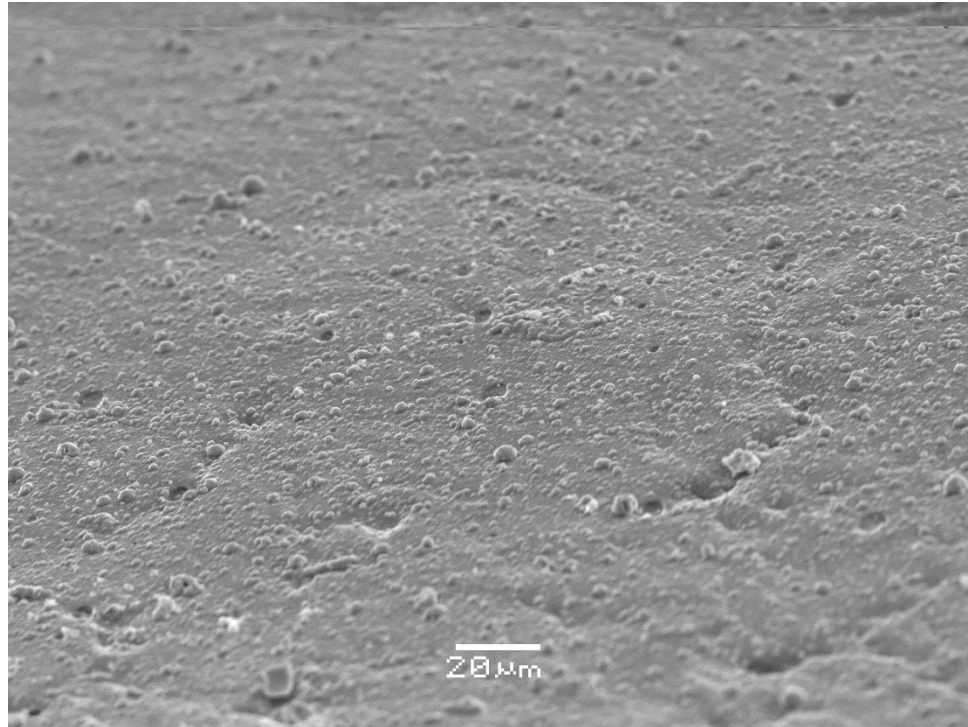


Figure B-15. TiN Thread Wall

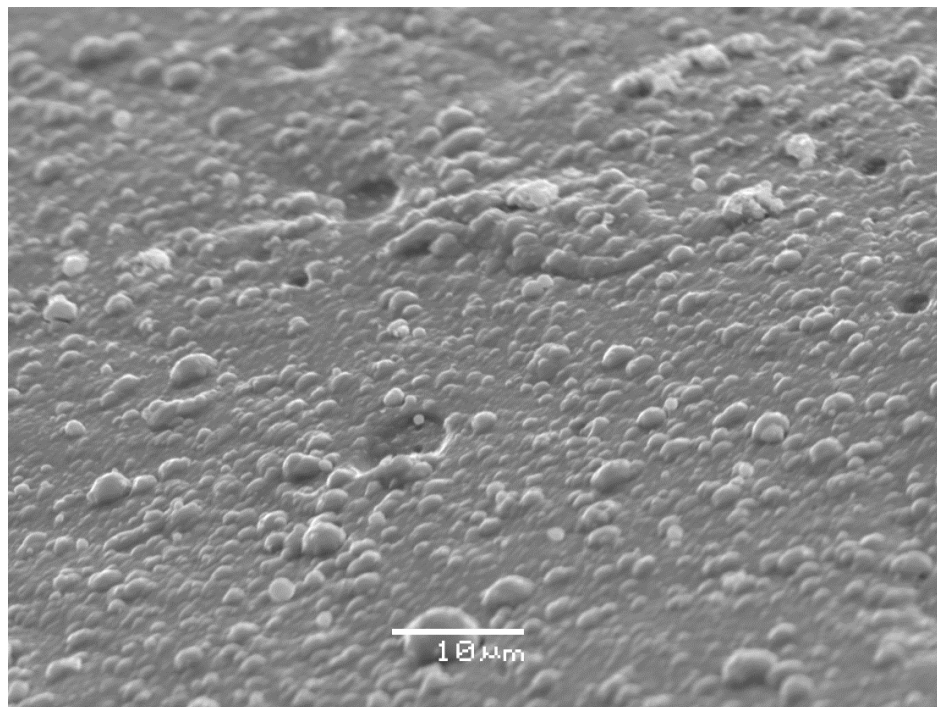


Figure B-16. TiN Thread Wall Close-up

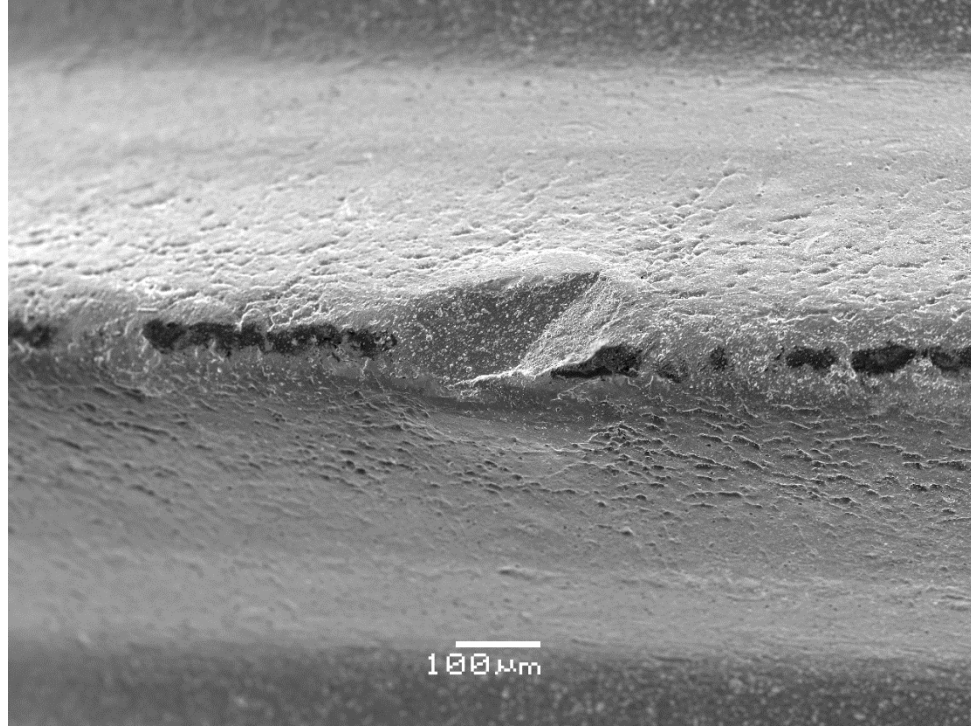


Figure B-17. TiN Thread Deformity

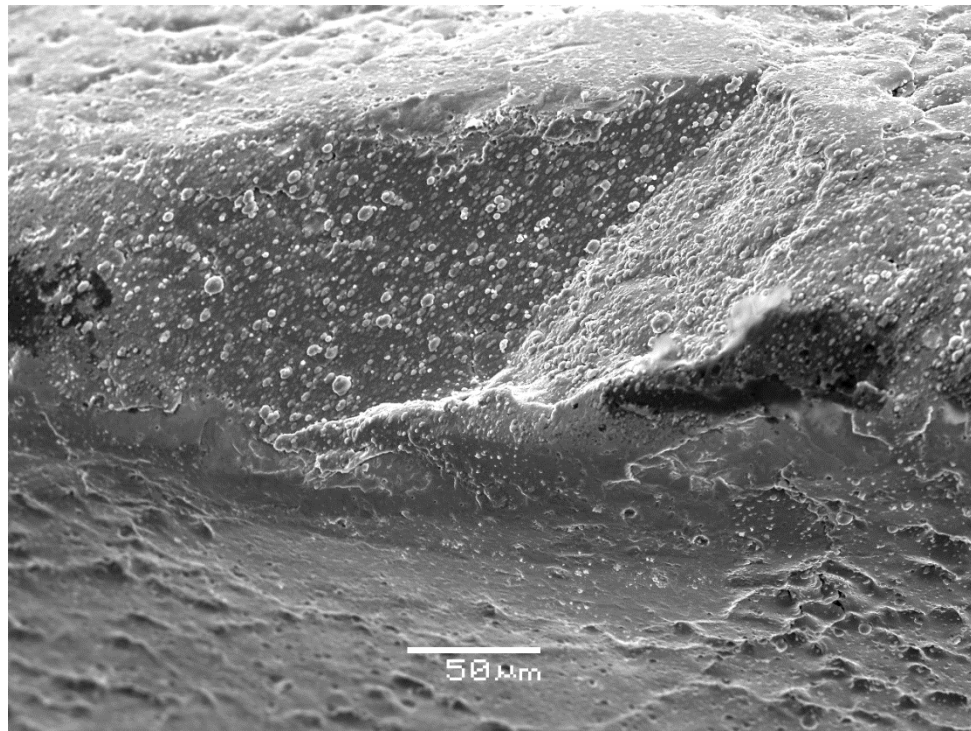


Figure B-18. TiN Thread Deformity Close-up

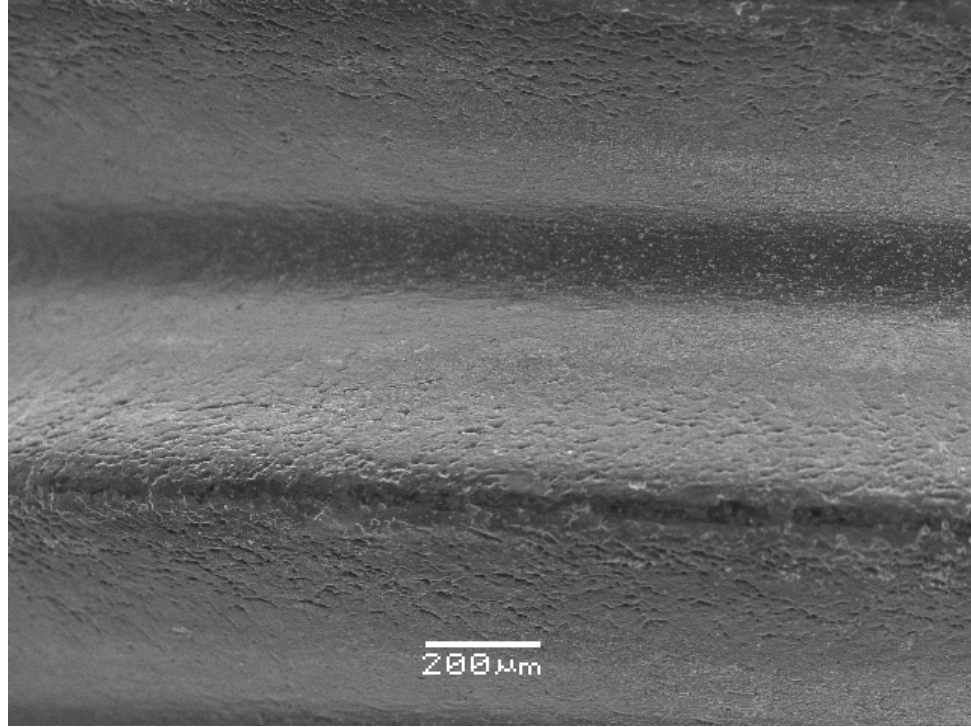


Figure B-19. TiN Thread

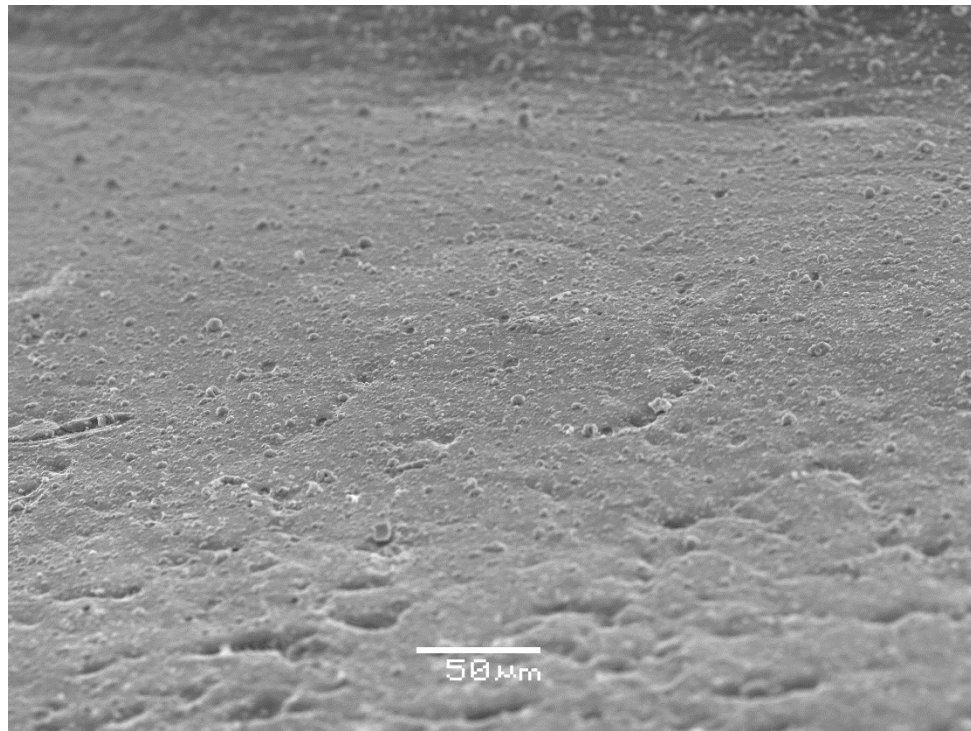


Figure B-20. TiN Thread Close-up

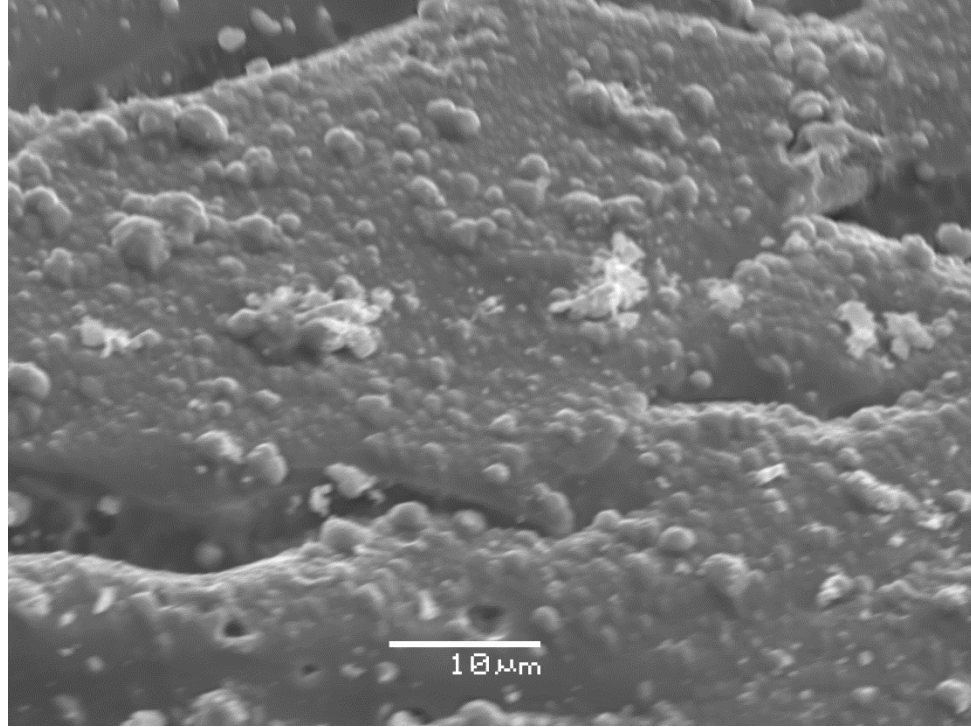


Figure B-21. TiN with Stainless Steel Wear Particles